Online Estimation of Power System Distribution Factors—A Sparse Representation Approach

Yu Christine Chen, Alejandro D. Domínguez-García, and Peter W. Sauer
Department of Electrical and Computer Engineering
University of Illinois at Urbana-Champaign
Urbana, Illinois 61801
Email: {chen267, aledan, psauer}@illinois.edu

***Abstract*—This paper proposes a method to compute linear sensitivity distribution factors (DFs) in near real-time without relying on a power flow model of the system. Instead, the proposed method relies on the solution of an underdetermined system of linear equations that arise from high-frequency synchronized measurements obtained from phasor measurement units. In particular, we exploit a sparse representation (i.e., one in which many elements are zero) of the desired DFs obtained via a linear transformation, and cast the estimation problem as an l_0-norm minimization. As we illustrate through examples, the proposed approach is able to provide accurate DF estimates with fewer sets of synchronized measurements than earlier approaches that rely on the solution of an overdetermined system of equations via the least-squares errors method.**

I. Introduction

Power system operational reliability is monitored and maintained via online static and dynamic security assessment tools, which generally rely on a model of the system obtained offline [1]. In particular, static security assessment involves real-time N-1 contingency analysis, in which operators determine whether or not the system will meet operational reliability requirements in case of outage in any one particular asset (e.g., a generator or transmission line) and, in turn, whether or not corrective actions are required to ensure operation in a secure state [2]. With an up-to-date model of the system, operators can perform these analyses by repeatedly solving the nonlinear power flow equations. However, for a large power system with many contingencies to consider, this process could take prohibitively long periods of time. One way to gain computational speed in contingency analysis is to use an estimate of the current operating point together with linear distribution factors (DFs), such as injection shift factors (ISFs) and line outage distribution factors (LODFs), obtained from an approximate power flow model of the system (see, e.g., [3]). Recently, the use of LODFs under multiple-line outages has been studied to evaluate operational security during cascading outages [4], [5]. Existing approaches to computing DFs typically rely on the so-called DC approximations [6]; however, this method of computing DFs lacks the flexibility of adapting to changes in network topology or generation and load variations, which can all affect the actual linear sensitivities significantly, and in turn the results of the analyses that use them.

Conventional model-based online analysis tools are not ideal since the results depend on an accurate model with up-to-date network topology, which may not be available due to erroneous telemetry from remotely monitored circuit breakers. For example, in the 2011 San Diego blackout, operators could not detect that certain lines were overloaded or close to being overloaded because the system model was not up-to-date [1]. Furthermore, the results from such model-based studies may not be applicable if the actual system evolution does not match any predicted operating points due to unforeseen circumstances such as outages in external areas or unpredictable levels of renewable generation. Thus, traditional model-based techniques may no longer satisfy the needs of monitoring and protection tasks; therefore it is important to develop measurement-based power system monitoring tools that are adaptive to changes in operating point and topology. In this regard, phasor measurement units (PMUs) are an enabling technology for the development of such measurement-based monitoring tools. In this context, recent work has been done in the area of detecting line outages using PMU measurements [7]–[9]; however, such proposed approaches still largely rely on a model of the system and largely utilize the so-called DC approximation.

In [10], we proposed a method to estimate ISFs in near real-time without relying on a power flow model of the system. The core idea behind this method is to find the solution of a system of linear equations formulated using real power bus injection and line flow data obtained from PMU measurements. In [10], we assumed an overdetermined system, with more equations than unknown ISFs, and obtained the solution via linear least-squares errors (LSE) estimation. While the method is shown to be adaptable to system topology changes, the LSE problem formulation necessitates at least as many sets of synchronized measurements as unknown ISFs. For a large power system, such a requirement may not satisfy the requirements of, e.g., online contingency analysis tools, since power systems are constantly undergoing changes and operators often need to quickly determine whether or not the current system operation is secure. This paper extends the work in [10] by proposing a method to recover the ISF solution using fewer sets of measurements than unknown ISFs. To this end, we transform the ISFs into a sparse vector representation (i.e., one in which many elements are zero), solve for the sparse vector via optimization, and finally compute the original ISFs by applying the inverse transformation.

II. ISF Computation Approach

Distribution factors are linearized sensitivities used in contingency analysis and remedial action schemes [3]. A key distribution factor is the injection shift factor (ISF), which quantifies the redistribution of power through each transmission line in a power system following a change in generation or load on a particular bus in the system. In essence, the ISF captures the sensitivity of the flow through a line with respect to changes in generation or load. In this section, we first describe the approach to ISF estimation that we proposed in [10], highlighting its main drawback, followed by the alternative we are proposing in the current work.

A. ISF Estimation via Least-Squares Errors Estimation

The ISF of line $L_{k\text{-}l}$ (assume positive real power flow from bus k to l) with respect to bus i, denoted by $\Psi^i_{k\text{-}l}$, is a linear approximation of the sensitivity of the active power flow in line $L_{k\text{-}l}$ with respect to the active power injection at node i, with the slack bus defined and all other quantities constant. Let $P_i(t)$ and $P_i(t+\Delta t)$, respectively, denote the active power injection at bus i at times t and $t+\Delta t$, $\Delta t > 0$ and small. Define $\Delta P_i(t) = P_i(t+\Delta t) - P_i(t)$ and denote the change in active power flow in line $L_{k\text{-}l}$ resulting from $\Delta P_i(t)$ by $\Delta P^i_{k\text{-}l}(t)$. Then, based on the definition of ISF, it follows that

$$\Psi^i_{k\text{-}l} := \frac{\partial P_{k\text{-}l}}{\partial P_i} \approx \frac{\Delta P^i_{k\text{-}l}(t)}{\Delta P_i(t)}. \tag{1}$$

In order to obtain $\Psi^i_{k\text{-}l}$, we need $\Delta P^i_{k\text{-}l}(t)$, which is not readily available from PMU measurements. We assume that the net variation in active power through line $L_{k\text{-}l}$, denoted by $\Delta P_{k\text{-}l}(t)$, however, is available from PMU measurements. We express this net variation as the sum of active power variations in line $L_{k\text{-}l}$ due to active power injection variations at each bus i:

$$\Delta P_{k\text{-}l}(t) = \Delta P^1_{k\text{-}l}(t) + \cdots + \Delta P^n_{k\text{-}l}(t). \tag{2}$$

Equivalently, by substituting (1) into (2), we can rewrite (2) as

$$\Delta P_{k\text{-}l}(t) \approx \Delta P_1(t)\Psi^1_{k\text{-}l} + \cdots + \Delta P_n(t)\Psi^n_{k\text{-}l},$$

where $\Psi^i_{k\text{-}l} \approx \frac{\Delta P^i_{k\text{-}l}}{\Delta P_i}$, $i = 1, \ldots, n$. Suppose $m+1$ sets of synchronized measurements are available. Let $\Delta P_i[j] = P_i((j+1)\Delta t) - P_i(j\Delta t)$ and $\Delta P_{k\text{-}l}[j] = P_{k\text{-}l}((j+1)\Delta t) - P_{k\text{-}l}(j\Delta t)$, $j = 1, \ldots, m$; and define $\Delta P_{k\text{-}l} = [\Delta P_{k\text{-}l}[1], \ldots, \Delta P_{k\text{-}l}[j], \ldots, \Delta P_{k\text{-}l}[m]]^T$, $\Delta P_i = [\Delta P_i[1], \ldots, \Delta P_i[j], \ldots, \Delta P_i[m]]^T$. Let $\Psi_{k\text{-}l} = [\Psi^1_{k\text{-}l}, \ldots, \Psi^i_{k\text{-}l}, \ldots, \Psi^n_{k\text{-}l}]^T$; then, it follows that

$$\Delta P_{k\text{-}l} = \begin{bmatrix} \Delta P_1 & \cdots & \Delta P_i & \cdots & \Delta P_n \end{bmatrix} \Psi_{k\text{-}l}. \tag{3}$$

For ease of notation, let ΔP represent the $m \times n$ matrix $[\Delta P_1, \ldots, \Delta P_i, \ldots, \Delta P_n]$; then, the system in (3) can be compactly written as

$$\Delta P_{k\text{-}l} = \Delta P \Psi_{k\text{-}l}. \tag{4}$$

As we proposed in [10], if $m \geq n$, then (4) is an overdetermined system, and we can solve for $\Psi_{k\text{-}l}$ via LSE as follows:

$$\hat{\Psi}_{k\text{-}l} = (\Delta P^T \Delta P)^{-1} \Delta P^T \Delta P_{k\text{-}l}. \tag{5}$$

However, for a large system with many buses, it may not be prudent to require such a large number of datasets before an estimate can be computed. Further, the adaptability of the measurement-based approach would be improved if fewer sets of data are required. Thus, in this paper, we focus on the problem of solving for $\Psi_{k\text{-}l}$ in (4) when $m < n$, i.e., obtaining a solution when (4) is an underdetermined system of equations.

B. ISF Estimation Algorithm

This work is inspired by the field of compressive sensing (see, e.g., [11]) and its applications to image processing, where a typical problem is to compress a large image (i.e., to reduce irrelevant or redundant image data in order to store or transmit the image efficiently), and subsequently reconstruct the image from its compressed representation. [Recently, compressive sensing (CS) ideas have been applied to the identification of multiple line outages in power systems [8].] CS theory asserts that, by exploiting their sparsity, certain classes of signals can be recovered from fewer samples or measurements than those needed in traditional methods such as LSE (see, e.g., [12], [13]). Specifically, the problem of recovering a sparse signal can be cast as an optimization problem where the objective is to minimize the l_0-norm[1] of the signal to be recovered.

In our setting, the signal of interest, the ISF vector $\Psi_{k\text{-}l}$, is not necessarily sparse; therefore, we search for an appropriate linear coordinate transformation M that results in a sparse $c_{k\text{-}l}$, such that $\Psi_{k\text{-}l} = Mc_{k\text{-}l}$. Assuming that such a sparse representation exists and since $c_{k\text{-}l}$ is sparse, it is intuitive to recover $c_{k\text{-}l}$ from knowledge of $\Delta P_{k\text{-}l}$ by solving

$$\begin{aligned} &\min_{c_{k\text{-}l}} ||c_{k\text{-}l}||_0, \\ &\text{subject to } \Delta P_{k\text{-}l} = \Delta P M c_{k\text{-}l}, \end{aligned} \tag{6}$$

where $||c_{k\text{-}l}||_0$ denotes the number of nonzero elements in $c_{k\text{-}l}$.

The problem in (6) is NP-hard due to the unavoidable combinatorial search [11]. There are numerous classes of computational techniques for solving sparse approximation problems. One such technique involves the relaxation of the l_0-norm minimization to an l_1-norm minimization [14]. The main idea behind CS is to exploit the equivalence of the l_0-minimization with the l_1-norm minimization, which is convex, when the dimension of $c_{k\text{-}l}$ is large [15]. Replacing the l_0-norm with the l_1-norm in (6), we get

$$\begin{aligned} &\min_{c_{k\text{-}l}} ||c_{k\text{-}l}||_1, \\ &\text{subject to } \Delta P_{k\text{-}l} = \Delta P M c_{k\text{-}l}. \end{aligned} \tag{7}$$

Many CS results revolve around conditions under which (6) and (7) are equivalent.

[1] For a vector with finite support, the l_0-norm is defined as the number of its entries that are nonzero (see, e.g., [11]).

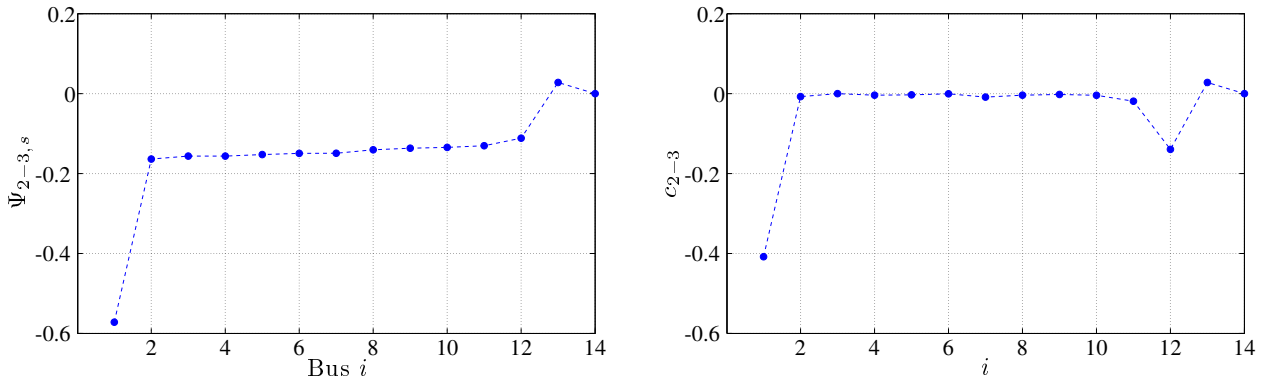

(a) Reordered ISFs but not sparse.

(b) Sparse signal after difference transformation.

Fig. 1: IEEE 14-bus system: ISFs of line $L_{2\text{-}3}$ with respect to each node pre-and post-transformation.

As mentioned earlier, the signal of interest in our setting is the vector of ISFs, $\Psi_{k\text{-}l}$, which may not be inherently sparse. In fact, it is hardly a "natural" signal, in the sense that the elements are ordered based on arbitrary indices defined by either the network diagram used in simulations or by the identification tags of PMUs in the field. Thus, in order to "sparsify" $\Psi_{k\text{-}l}$, we first rearrange the elements of $\Psi_{k\text{-}l}$ in order of decreasing magnitude, and then we apply the *difference transformation* (to be defined below) to the sorted signal. This leads to a sparse representation of the ISFs, which in turn casts the ISF estimation problem into a sparse vector estimation problem.

1) Sparsifying the ISF Vector: We assume that, prior to online estimation, $\Psi_{k\text{-}l}$ was computed either by model-based studies or by linear least-squares estimation as in [10]. We next sort and rearrange the elements in $\Psi_{k\text{-}l}$ in order of decreasing magnitude, and denote this rearranged vector as $\Psi_{k\text{-}l,s}$, i.e.,

$$\Psi_{k\text{-}l,s} = [\Psi^1_{k\text{-}l,s}, \ldots, \Psi^i_{k\text{-}l,s}, \ldots, \Psi^n_{k\text{-}l,s}]^T,$$

such that $|\Psi^i_{k\text{-}l,s}| \geq |\Psi^j_{k\text{-}l,s}|$ for all $i \leq j$. The sorted signal, $\Psi_{k\text{-}l,s}$, is assumed to be a relatively smooth signal with only a few sharp edges, so the difference between consecutive elements is likely small; this is the premise upon which we build a sparse representation of $\Psi_{k\text{-}l,s}$, and subsequently estimate $\Psi_{k\text{-}l}$.

While $\Psi_{k\text{-}l,s}$ may be characterized by smooth segments separated by sporadic jumps after reordering of the nodes based on magnitude, it still retains the same level of sparsity as $\Psi_{k\text{-}l}$. However, it may be possible to find a linear transformation that results in a sparse representation of $\Psi_{k\text{-}l,s}$; next we define one such transformation. This transformation is defined via the difference between consecutive elements of $\Psi_{k\text{-}l,s}$:

$$c^i_{k\text{-}l} = \Psi^i_{k\text{-}l,s} - \Psi^{i+1}_{k\text{-}l,s}, \quad c^n_{k\text{-}l} = \Psi^n_{k\text{-}l,s}. \tag{8}$$

In matrix form, the *difference transformation*, defined in (8), can be written as

$$c_{k\text{-}l} = M^{-1}\Psi_{k\text{-}l,s},$$

where

$$M^{-1} = \begin{bmatrix} 1 & -1 & 0 & 0 & \ldots & 0 \\ 0 & 1 & -1 & 0 & \ldots & 0 \\ \vdots & \vdots & \ddots & \ddots & \vdots & \vdots \\ 0 & 0 & 0 & 1 & -1 & 0 \\ 0 & 0 & 0 & 0 & 1 & -1 \\ 0 & 0 & 0 & 0 & 0 & 1 \end{bmatrix}. \tag{9}$$

If this difference transformation, indeed, results in $c_{k\text{-}l}$ being sparse, we can then exploit the equivalence of l_1-norm and l_0-norm minimizations to compute the estimate $\hat{c}_{k\text{-}l}$ and then apply the inverse difference transformation to obtain the estimate $\hat{\Psi}_{k\text{-}l}$. Next, we illustrate the effectiveness of the difference transformation in (9) for sparsifying an ISF vector.

Example 1 (IEEE 14-Bus System): Consider the IEEE 14-bus system [16]. We compute the model-based linear sensitivity ISF vector of line $L_{2\text{-}3}$, $\Psi_{2\text{-}3}$, using the partial derivative definition in (1). These are the benchmark values to which we compare any estimation results in the remainder of the paper. In Fig. 1a, we plot these model-based ISFs after sorting by the magnitude of each element. While the rearranged signal is fairly smooth except at buses 1, 12, and possibly 13, this vector only has one zero element (at bus 14). In order to obtain a sparse representation, we apply the difference transformation to the signal shown in Fig. 1a and obtain the signal depicted in Fig. 1b, which contains many zero or near-zero elements with the same sharp edges as in Fig. 1a. ■

2) Minimizing the l_1-Norm: Through sorting and transforming the original ISF vector $\Psi_{k\text{-}l}$, we assume the post-transformation signal $c_{k\text{-}l}$ to be sparse (this was illustrated in Example 1). Since the elements of $\Psi_{k\text{-}l}$ has been sorted by magnitude, we also rearrange the columns of ΔP accordingly and denote this reordered matrix as ΔP_s. We now solve for an estimate for $c_{k\text{-}l}$ as $\arg\min ||c_{k\text{-}l}||_0$, which can be relaxed to the convex program in (7). Let $\Delta P_{k\text{-}l}[j]$ and $\Delta P_s[j]$ denote the j^{th} element of $\Delta P_{k\text{-}l}$ and the j^{th} row of ΔP_s, respectively. We then relax the equality constraint in (7) to element-wise inequality constraints and obtain the following

TABLE I: Comparison of $\hat{c}_{2\text{-}3}$ obtained in Example 2.

i	$c^i_{2\text{-}3}$	$\hat{c}^i_{2\text{-}3}$ (via l_1-minimization)		$\hat{c}^i_{2\text{-}3}$ (via LSE)	
		$m = 10$	$m = 13$	$m = 14$	$m = 20$
1	-0.4082	-0.4172	-0.4105	-0.4124	-0.4080
2	-0.0074	0	-0.0050	-0.0020	-0.0069
3	0	0	0	-0.0025	0.0001
4	-0.0039	-0.0055	-0.0038	-0.0009	-0.0041
5	-0.0030	-0.0044	-0.0033	-0.0070	-0.0013
6	-0.0004	0	0	0.0002	-0.0011
7	-0.0087	0	-0.0074	0.0002	-0.0118
8	-0.0039	-0.0093	-0.0062	-0.0104	-0.0021
9	-0.0021	0	-0.0005	-0.0018	-0.0011
10	-0.0041	-0.0016	-0.0030	-0.0022	-0.0050
11	-0.0189	-0.0171	-0.0182	-0.0169	-0.0189
12	-0.1394	-0.1415	-0.1400	-0.1417	-0.1393
13	0.0279	0.0242	0.0265	0.0273	0.0279
14	0	-0.0017	-0.0005	-0.0017	0.0003
$\|\|\hat{c}_{2\text{-}3} - c_{2\text{-}3}\|\|_2$		0.0167	0.0050	0.0147	0.0043

TABLE II: Comparison of $\hat{\Psi}_{2\text{-}3,s}$ obtained in Example 3.

i	$\Psi^i_{2\text{-}3,s}$	$\hat{\Psi}^i_{2\text{-}3,s}$ (via l_1-minimization)		$\hat{\Psi}^i_{2\text{-}3,s}$ (via LSE)	
		$m = 10$	$m = 13$	$m = 14$	$m = 20$
1	-0.5719	-0.5740	-0.5720	-0.5720	-0.5713
2	-0.1637	-0.1569	-0.1614	-0.1596	-0.1633
3	-0.1563	-0.1569	-0.1564	-0.1575	-0.1564
4	-0.1563	-0.1569	-0.1564	-0.1550	-0.1565
5	-0.1524	-0.1514	-0.1527	-0.1541	-0.1524
6	-0.1494	-0.1469	-0.1493	-0.1471	-0.1511
7	-0.1491	-0.1469	-0.1493	-0.1473	-0.1500
8	-0.1404	-0.1469	-0.1419	-0.1475	-0.1381
9	-0.1366	-0.1376	-0.1358	-0.1371	-0.1360
10	-0.1345	-0.1376	-0.1353	-0.1353	-0.1350
11	-0.0189	-0.1361	-0.1322	-0.1331	-0.1300
12	-0.1115	-0.1190	-0.1140	-0.1162	-0.1111
13	0.0279	0.0225	0.0260	0.0255	0.0282
14	0	-0.0017	-0.0005	-0.0017	0.0003
$\|\|\hat{\Psi}_{2\text{-}3,s} - \Psi_{2\text{-}3,s}\|\|_2$		0.0154	0.0048	0.0110	0.0032

l_1-norm minimization problem:

$$\arg\min_{c_{k\text{-}l}} ||c_{k\text{-}l}||_1, \tag{10}$$
$$\text{subject to } |\Delta P_{k\text{-}l}[j] - \Delta P_s[j] M c_{k\text{-}l}| < \epsilon,\ j = 1, \ldots, m,$$

where $\epsilon > 0$ and small. Next, we illustrate the ideas above via an example.

Example 2 (IEEE 14-Bus System): Here, we consider the same system as in Example 1. In order to simulate PMU measurements of slight fluctuations in active power injection at each bus, we create power injection times-series data. The injection at bus i, denoted by P_i, is

$$P_i[j] = P_i^0[j] + \sigma_1 P_i^0[j] v_1 + \sigma_2 v_2, \tag{11}$$

where $P_i^0[j]$ is the nominal power injection at bus i at instant j, and v_1 and v_2 are pseudorandom values drawn from standard normal distributions with 0-mean and standard deviations $\sigma_1 = 0.1$ and $\sigma_2 = 0.1$, respectively. The first component of variation, $\sigma_1 P_i^0[j] v_1$, represents the inherent fluctuations in generation and load, while the second component, $\sigma_2 v_2$, represents random measurement noise. For each set of bus injection data, we compute the power flow, with the slack bus absorbing all power imbalances, and the active power flow through each line for that particular time.

With the dataset generated from the procedure above, we apply (10) to compute estimates of $c_{2\text{-}3}$, denoted as $\hat{c}_{2\text{-}3}$, for several values of $m < n$. These are shown in columns 3 and 4 of Table I for $m = 10, 13$, respectively. The model-based benchmark transformed ISFs, $c_{2\text{-}3}$, are listed in column 2 (and also plotted in Fig. 1b). Finally, we sparsify the LSE-based ISF vector estimate that results from (5) by using 14 and 20 sets of measurements; and we list the elements of the transformed signals in columns 5 and 6 in Table I, for $m = 14, 20$, respectively. By inspecting this table, we conclude that the LSE-based approach with $m = 14$ is less accurate than the l_1-norm minimization with $m = 10$ and $m = 13$, which is verified by comparing the l_2-norm of the error in each estimate as compared to the benchmark model-based $c_{2\text{-}3}$, as shown in the last row. However, we note that the LSE solution with $m = 20$ is more accurate than the l_1-norm minimization ones, and therefore there is some tradeoff between the accuracy level obtained and the number of measurements required. ■

3) Reconstructing the ISF Estimate: Let $\hat{\Psi}_{k\text{-}l,s}$ denote the estimate for $\Psi_{k\text{-}l,s}$. Once the estimate $\hat{c}_{k\text{-}l}$ is obtained, we apply the inverse difference transformation to obtain $\hat{\Psi}_{k\text{-}l,s}$ as follows:

$$\hat{\Psi}_{k\text{-}l,s} = M \hat{c}_{k\text{-}l}, \tag{12}$$

where

$$M = \begin{bmatrix} 1 & 1 & 1 & 1 & \ldots & 1 \\ 0 & 1 & 1 & 1 & \ldots & 1 \\ \vdots & \vdots & \ddots & \ddots & \vdots & \vdots \\ 0 & 0 & 0 & 1 & 1 & 1 \\ 0 & 0 & 0 & 0 & 1 & 1 \\ 0 & 0 & 0 & 0 & 0 & 1 \end{bmatrix}.$$

Example 3 (IEEE 14-Bus System): Continuing with Example 2, we apply the inverse difference transformation M to each $\hat{c}_{2\text{-}3}$ to obtain $\hat{\Psi}_{2\text{-}3}$ for $m = 10, 13$; the results are shown in columns 3 and 4 in Table II, respectively. The model-based benchmark ISFs, $\Psi^i_{2\text{-}3}$, $i = 1, \ldots, 14$, are listed in column 2 (and also plotted in Fig. 1a). Further, in columns 5 and 6, we show the ISF vectors resulting from the LSE solution in (5). Again, the normed error shown the bottom row of Table II indicates that the l_1-norm minimization achieves higher accuracy with $m = 10, 13$ than the LSE solution with $m = 14$, but not with $m = 20$. Optionally, we may also rearrange $\hat{\Psi}_{k\text{-}l,s}$ back into the original index order, denoted as $\hat{\Psi}_{k\text{-}l}$, which is an estimate for $\Psi_{k\text{-}l}$. ■

III. Case Study

In this section, we further illustrate the concepts presented in Section II using the NPCC 48-machine system, which contains 140 buses [17]. For this case study, we focus on the ISFs of line $L_{53\text{-}51}$ with respect to each bus, and denote the corresponding ISF vector by $\Psi_{53\text{-}51}$. We compute its benchmark value using the definition of the ISF in (1), which we plot in Fig. 2a. This original vector, ordered by the somewhat arbitrary network diagram designation, is neither sparse nor particularly smooth. Next, we reorder the elements of $\Psi_{53\text{-}51}$ by the magnitude of its entries to get $\Psi_{53\text{-}51,s}$, which contains large smooth segments with a few sharp edges. We then apply the difference transformation described in Section II-B1 to $\Psi_{53\text{-}51,s}$ and obtain $c_{53\text{-}51}$, as shown in Fig. 2b.

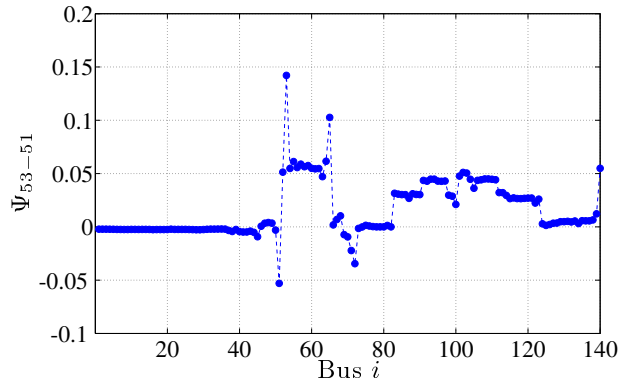

(a) Nodes ordered by network diagram designation.

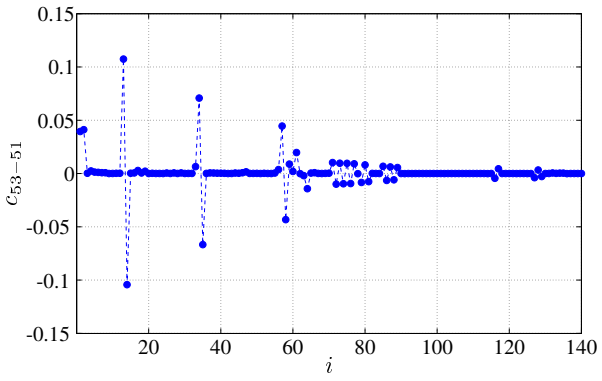

(b) Sparse signal after difference transformation.

Fig. 2: NPCC 48-machine system: ISFs of line $L_{53\text{-}51}$ with respect to each node pre-and post-transformation.

TABLE III: Comparison of errors in $\hat{\Psi}_{53\text{-}51}$ ($||\hat{\Psi}_{53\text{-}51} - \Psi_{53\text{-}51}||_2$) for NPCC system.

l_1-minimization					LSE
$m = 59$	$m = 79$	$m = 99$	$m = 119$	$m = 139$	$m = 140$
0.0790	0.0289	0.0186	0.0045	0.0026	0.0310

By visual inspection, we note that $c_{53\text{-}51}$ is, indeed, a sparse vector and we may take advantage of l_1-norm minimization to obtain an estimate for the ISFs with $m < n$ sets of measurements. We apply the optimization approach in (10) with $m = 59, 79, 99, 119, 139$ to obtain $\hat{c}_{53\text{-}51}$ in each case. We then transform the sparse signal back into estimates for the ISF vector, $\hat{\Psi}_{53\text{-}51}$, and compute the normed error of each estimate away from the benchmark model-based ISF vector (see Table III). Furthermore, we compute the error for the ISF vector obtained from LSE with $m = 140$. It is evident, by inspecting Table III, that the l_1-norm minimization with as few as 79 measurements (nearly half that of the LSE approach) produces an estimate for the ISF vector that is more accurate than the LSE approach with 140 measurements.

IV. Concluding Remarks

In this paper, we presented a method to estimate a vector of ISFs by exploiting a sparse representation of it, and solving for the sparse vector via l_0-norm minimization. An advantage of the method is that it does not rely on a power flow model of the system, bus instead only uses PMU measurements collected in real-time. Apart from eliminating the power flow model, we show that the proposed measurement-based approach provides accurate estimates of the ISFs using fewer measurements than those obtained using LSE.

Beyond the l_1-norm convexification approach, further work includes investigation of the advantage of using greedy algorithms, to improve the computation time involved in the optimization. Another avenue for future work would be to devise algorithms that estimate the DFs accurately in the presence of corrupted measurements.

References

[1] FERC and NERC. (2012, Apr.) Arizona-southern california outages on september 8, 2011: Causes and recommendations. [Online]. Available: http://www.ferc.gov/legal/staff-reports/04-27-2012-ferc-nerc-report.pdf

[2] U.S.-Canada Power System Outage Task Force. (2004, Apr.) Final report on the august 14th blackout in the united states and canada: causes and recommendations. [Online]. Available: https://reports.energy.gov/BlackoutFinal-Web.pdf

[3] A. Wood and B. Wollenberg, *Power Generation, Operation and Control*. New York: Wiley, 1996.

[4] T. Güler, G. Gross, and M. Liu, "Generalized line outage distribution factors," *IEEE Transactions on Power Systems*, vol. 22, no. 2, pp. 879–881, 2007.

[5] J. Guo, Y. Fu, Z. Li, and M. Shahidehpour, "Direct calculation of line outage distribution factors," *IEEE Transactions on Power Systems*, vol. 24, no. 3, pp. 1633 – 1634, 2009.

[6] B. Stott, J. Jardim, and O. Alsac, "Dc power flow revisited," *IEEE Transactions on Power Systems*, vol. 24, no. 3, pp. 1290 – 1300, 2009.

[7] J. E. Tate and T. J. Overbye, "Line outage detection using phasor angle measurements," *IEEE Transactions on Power Systems*, vol. 23, no. 4, pp. 1644 – 1652, 2008.

[8] H. Zhu and G. B. Giannakis, "Sparse overcomplete representations for efficient identification of power line outages," *IEEE Transactions on Power Systems*, vol. 27, no. 4, pp. 2215 – 2224, 2012.

[9] R. Emami and A. Abur, "External system line outage identification using phasor measurement units," *IEEE Transactions on Power Systems*, vol. 28, no. 2, pp. 1035–1040, 2013.

[10] Y. C. Chen, A. D. Domínguez-García, and P. W. Sauer, "Online computation of power system linear sensitivity distribution factors," in *Proc. of the IREP Bulk Power System Dynamics and Control Symposium*, August 2013.

[11] Y. C. Eldar and G. Kutyniok, *Compressed sensing: theory and applications*. Cambridge University Press, 2012.

[12] D. L. Donoho, "Compressed sensing," *IEEE Transactions on Information Theory*, vol. 52, no. 4, pp. 1289 – 1306, 2006.

[13] E. J. Candès, J. Romberg, and T. Tao, "Robust uncertainty principles: Exact signal reconstruction from highly incomplete frequency information," *IEEE Transactions on Information Theory*, vol. 52, no. 2, pp. 489 – 509, 2006.

[14] J. Tropp and S. Wright, "Computational methods for sparse solution of linear inverse problems," *Proceedings of the IEEE*, vol. 98, no. 6, pp. 948–958, jun 2010.

[15] R. Baraniuk, "Compressive sensing," *IEEE Signal Processing Magazine*, vol. 24, no. 4, pp. 118 – 121, july 2007.

[16] University of Washington. (2012, Oct.) Power system test case archive. [Online]. Available: http://www.ee.washington.edu/research/pstca/

[17] J. Chow and K. Cheung, "A toolbox for power system dynamics and control engineering education and research," *IEEE Transactions on Power Systems*, vol. 7, no. 4, pp. 1559 –1564, Nov. 1992.